IEEE Access
Multidisciplinary ⋮ Rapid Review ⋮ Open Access Journal

Received 15 August 2022, accepted 11 September 2022, date of publication 15 September 2022,
date of current version 29 September 2022.

Digital Object Identifier 10.1109/ACCESS.2022.3206845

RESEARCH ARTICLE

An Augmented Lever Analogy Method for Kinematic Analysis of Dual-Input Planetary/Epicyclic Gear Sets Involving Planet Gear

XIAODONG YANG[1,2], WENNIAN YU[1,2], YIMIN SHAO[1], ZHILIANG XU[1,2], QIANG ZENG[1], CHUNHUI NIE[1,2], AND DINGQIANG PENG[1,2]

[1]State Key Laboratory of Mechanical Transmission, Chongqing University, Chongqing 400044, China
[2]College of Mechanical and Vehicle Engineering, Chongqing University, Chongqing 400044, China

Corresponding author: Wennian Yu (wennian.yu@cqu.edu.cn)

This work was supported by the National Natural Science Foundation of China under Grant 52035002 and Grant 52105086, and in part by the China Postdoctoral Science Foundation under Grant 2021M700583.

ABSTRACT The lever analogy method (LAM) is a translational system representation for the rotating components and is widely used for the kinematic analysis of PGSs/EGSs. However, it includes only the sun gear, ring gear, and carrier, and ignores the kinematic information of the planet gear. The planet gear kinematic information is vital for its bearing life prediction, and speed sequence, power flow, and efficiency analysis of dual-input PGSs/EGSs. The traditional LAM doesn't work when involving the planet gear kinematic information, because the kinematic information of planet gear is eliminated during the process of merging similar items. In this paper, an augmented lever analogy method (ALAM) is proposed to make up for the lack of traditional LAM in analyzing planet gear kinematic information, and analyze the kinematic relationship between planet gear to other components for the dual-input PGSs/EGSs. In this method, the new nodes and lever lengths representing the planet gear are added to the LAM by analyzing peripheral velocity relationships at the meshing points of PGSs/EGSs. In addition, not all the dual-input compound PGSs/EGSs (e.g. the compound PGSs/EGSs with planet gears in series, etc.) can be analyzed by the traditional LAM. The proposed method can easily establish the augmented lever models for all of them and derive the corresponding kinematic expressions. The results show that the proposed ALAM has good visibility and greater versatility, and can accurately and efficiently calculate the rotating speed of planet gears for calculating the speed sequence, power flow, and efficiency of PGSs/EGSs, which can cover all kinds of the PGSs/EGSs, and greatly reduce the technical threshold and time for their kinematic analysis.

INDEX TERMS Planetary gear set, planet gear, speed sequence, lever analogy method, dual-input.

NOMENCLATURE

PGSs/EGSs	Planetary/Epicyclic gear sets
LAM	Lever analogy method
ALAM	Augmented lever analogy method
ω_{Ratio}	The ratio between the rotating speed
EVT	Electrical variable transmission
SPGS	Simple planetary gear set
DPGS	Double-planet planetary gear set
PGS-i	First PGS (Front), $i = 1$; Second PGS (Rear), $i = 2$.
Z_j	The teeth number of component j, $j = S, R, P$.
K	The characteristic parameter of PGS, $K = Z_R/Z_S$.
T_k	The load torque of component k, $k = S, R, P, C$.
ω_k	The rotating speed of component k, $k = S, R, P, C$.

The associate editor coordinating the review of this manuscript and approving it for publication was Gongbo Zhou.

This work is licensed under a Creative Commons Attribution 4.0 License. For more information, see https://creativecommons.org/licenses/by/4.0/

L_q	The lever length of planet gear q, $q = P$ (SPGS); $q = P1$, $P2$ (DPGS); $q = b$ (rolling bearing)
S+S	A 2PGS arrangement with its first (PGS-1) and second (PGS-2) gear set both being SPGS
S+D	A 2PGS arrangement with its first (PGS-1) and second (PGS-2) gear set being SPGS and DPGS respectively
D+S	A 2PGS arrangement with its first (PGS-1) and second (PGS-2) gear set being DPGS and SPGS respectively
D+D	A 2PGS arrangement with its first (PGS-1) and second (PGS-2) gear set both being DPGS
$R^k_{i,j}$	The speed ratio between components i and j relative to the component k.
S, R, P, C	Sun gear, Ring gear, Planet gear and Carrier
R-C	Ring gear and carrier dual-input working condition

I. INTRODUCTION

Planetary/Epicyclic gear sets (PGSs/EGSs) have the advantages of high transmission ratios, large torque-weight ratios and compactness in comparison with ordinary gear trains, which make them widely used in fields like automotive, aerospace, marine, wind turbines, and machine tools applications [1], [2], [3]. Currently, a lot of methods have been proposed for the design and kinematic analysis of PGSs/EGSs, such as the component analysis synthesis method, the line graph synthesis method, the combination solution method, the rod system conversion [4], and the lever analogy method (LAM) [5], etc. The component analysis synthesis method and the combined solution method are traditional methods of analyzing PGSs/EGSs. However, a large number of kinematic equations need to be established when applying these methods which makes them cumbersome and lacks universality. The line graph synthesis method, the rod system conversion, and the LAM are graph-based methods. Applying the graph theory to the kinematic analysis of PGSs/EGSs, a simple and practical LAM was first proposed by Benford and Leising [5], which considers the PGS as an equivalent vertical lever based on appropriate assumption and simplification to position PGS. The vertical lever equivalent substitution reflects the characteristics so that the position relationship of PGS rotating members can be reflected faithfully. This makes the analysis of complex planetary transmission mechanisms easy and general [6].

Due to the advantages of the LAM, it is widely used to facilitate the transmission analysis of complex PGS mechanisms, especially for automotive automatic transmission, e.g. electrical variable transmissions (EVTs). Ahn *et al.* [7] used the LAM to analyze the maximum speed for the performance investigation of a dual-mode EVT. The torque and speed of the powertrain elements and power split ratio were analyzed using the LAM by Wang *et al.* [8] and Kim *et al.* [9]. Barhoumi *et al.* [10], Barhoumi *et al.* [11], Kim and Kum[12], and Kang *et al.* [13] used the LAM to explore fuel economy and acceleration performance metrics, of compound split hybrid configurations. Yang *et al.* [14] analyzed the configurations and upshift/downshift process kinematics of the dual-input compound power-split mechanism (DICPSM). Liu *et al.* [15] proposed a systematic design method to synthesize the configuration scheme for multi-row and multi-speed AT based on the LAM. Xie *et al.* [16] analyzed the speed ratio of components by using the lever analogy method to derive the two-PGS PGTs with a high reduction speed ratio. Zhang *et al.* [17] obtained eight schemes with a high reduction speed ratio based on the LAM. Liao and Chen [1] presented an improved lever analogy method to simplify the analysis for determining the speed ratios for automatic transmissions based on the LAM. The LAM is used to analyze the speed of the components of PGSs/EGSs in the above research. Additionally, the other properties researches of PGSs/EGSs transmissions, such as the power flow, torque, and configuration, are using the LAM to analyze the components' speed. Chao *et al.* [18] and Hong *et al.* [19] studied the power flow of series-split EVT for a plug-in hybrid vehicle by using the LAM. Zhu *et al.* [20] used the LAM to analyze the transient torques with different power sources for a multi-mode transmission with a single electric machine. Ho and Hwang [21] applied the graph theory and the LAM to analyze the power flow, kinematic, and configurations of PGSs/EGSs. Ross and Route [22] established compound levers consisting of multiple levers in parallel connection by considering the number and magnitude of the required ratios. Liu *et al.* [23] proposed a systematic analysis methodology to design suitable three-mode configurations based on the lever model. Based on a deduction method and composite lever analogy, Peng *et al.* [24] developed an efficient synthesis method for the PGS with two operating DOFs.

The above research analyzed the rotating speed of ring gear, carrier, and sun gear based on the LAM, but that of planet gear cannot be obtained since traditional LAM ignores the kinematic information of planet gear. However, the rotating speed and other kinematic information of planet gear are necessary in cases, such as the power flow and efficiency analysis for dual-input PGSs/EGSs [25], [26], mesh phasing relationships analysis [2], [27], entrainment velocity of ball bearings and PGSs/EGSs [28], [29], [30], [31] and the limit speed and life span of bearing ball and planet gear as the design limitation factors [32]. Therefore, based on the advantages of the LAM, an innovative method, which exceeds the research limitation of the traditional LAM, is urgently needed to establish the general lever model for all kinds of PGSs/EGSs and analyze their kinematic information. In this paper, an extended lever analogy method (ALAM) containing the kinematic information of planet gears is proposed. In this method, the three instantaneous centers theorem is used to establish the kinematic equations among components

of PGSs/EGSs, which can create the new lever relationships of planet gear to other components. This method can form the 4-node and 5-node lever models for the simple planetary gear set (SPGS) and double-planet planetary gear set (DPGS), respectively, without rederiving the complex kinematic equation set. Therefore, based on the proposed ALAM, the compound lever models for all kinds of the PGSs/EGSs mechanisms including compound PGSs/EGSs with planet gears in series can be established by including the planet gear to intuitively and efficiently calculate the rotating speed of the planet gears, and to derive the kinematic relationship expressions for all components of the PGSs/EGSs. This makes up for the lack in analyzing kinematic of planet gear and the compound PGSs/EGSs with planet gears in series of the traditional LAM as it eliminates the kinematic information of planet gear during the process of merging similar items. Thus, the proposed ALAM is an efficient and universal method for the kinematic analysis of the PGSs/EGSs mechanisms.

The rest of this paper is organized as follows. In Section 2, the theoretical mechanism of the traditional LAM and the ALAM are derived by utilizing the three instantaneous centers theorem. In Section 3, the proposed ALAM is verified by taking an example of compound PGSs/EGSs with planet gears in series. In Section 4, the analysis models of dual-input for PGSs/EGSs are established based on the new lever models of the proposed method. In Section 5, the speed ratio relationships and speed sequence regions of all components in PGSs/EGSs under different working modes are calculated and discussed. Finally, conclusions are summarized in Section 6.

II. THE PROPOSED EXTENDED LEVER ANALOGY METHOD

A. THE TRADITIONAL LEVER ANALOGY METHOD

In order to reveal the reason for the lack of kinematics analysis of planet gear and the compound PGSs/EGSs with planet gears in series, and to provide a theoretical basis for the derivation of ALAM, the theoretical mechanisms of traditional LAM for the SPGS and DPGS are derived in this Section.

The structure type of PGSs includes the DPGS and the SPGS, which are widely used in the transmission system of the vehicle industry, such as the Ravigneaux planetary gear set. Their elementary lever models [17], [24] are shown in Fig. 1.

The LAM uses the vertical lever equivalent substitution to reflect the kinematic characteristics of PGSs/EGSs so that the position relationship of PGSs/EGSs rotating members can be reflected faithfully. This makes the analysis of complex PGSs/EGSs transmission mechanisms easy and general [5], [6]. However, the theoretical mechanism of the traditional LAM has not been revealed and the kinematic information of planet gear can not be analyzed by the LAM.

In this paper, the traditional lever model of the PGSs/EGSs is derived based on the Aronhold-Kennedy theorem of three instantaneous centers [34], which reveals the theoretical mechanism of LAM, and provides a theoretical basis for the

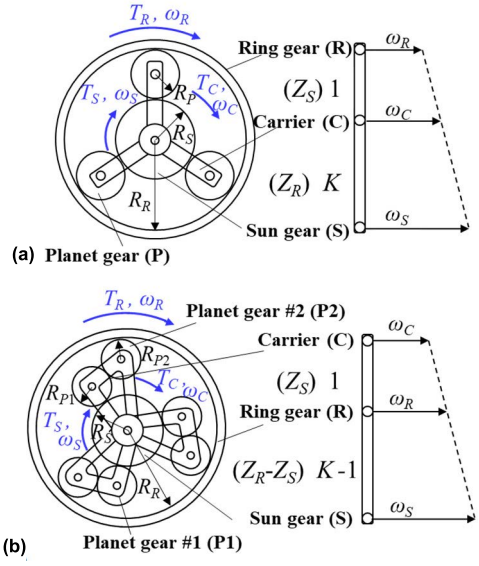

FIGURE 1. Mechanism diagrams and lever models of PGSs: (a) SPGS; (b) DPGS [12], [33].

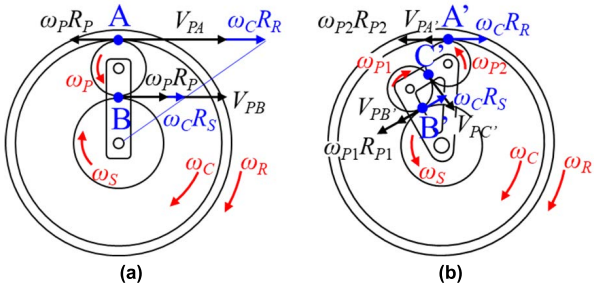

FIGURE 2. Kinematic model of a planetary gear set: (a) SPGS; (b) DPGS.

derivation of ALAM including the kinematic information of planet gear.

The kinematic models of SPGS and DPGS shown in Fig. 2 are used to analyze the kinematic relationships among three components, i.e. the sun gear, the ring gear, and the carrier. In Fig. 2 (a), R_P and ω_P represent the base circle radius and the rotating speed of the planet gear. Here, points A and B denote the meshing points of the ring-planet gear pair and the sun-planet gear pair of SPGS, respectively. Similarly, in Fig. 2 (b), R_{P1} and R_{P2} represent the base circle radius of planet gear #1 and planet gear #2, respectively. ω_{P1} and ω_{P2} represent the rotating speed of planet gear #1 and planet gear #2, respectively. Meanwhile, points A' and B' denote the meshing points of the ring-planet gear pair and the sun-planet gear pair of DPGS, respectively.

In Fig. 2 (a), the sun gear, the ring gear, and the carrier are rotating in the same direction, and the planet gear is rotating in the opposite direction. Therefore, the kinematic equations of the model in Fig. 2 (a) can be described as follows:

$$\begin{cases} V_{PA} = \omega_C R_R - \omega_P R_P \\ V_{RA} = \omega_R R_R \\ V_{PB} = \omega_C R_S + \omega_P R_P \\ V_{SB} = \omega_S R_S \end{cases} \tag{1}$$

where, V_{PB}, V_{SB} represent the peripheral velocity at point B of the planet gear and the sun gear of SPGS, respectively. V_{PA}, V_{RA} represent the peripheral velocity at point A of the planet gear and the ring gear of SPGS, respectively. Based on the identities $V_{PA} = V_{RA}$, $V_{PB} = V_{SB}$, so the equality of $V_{PA} + V_{PB} = V_{RA} + V_{SB}$ is established, and the following equation can be obtained:

$$\omega_S R_S + \omega_R R_R = \omega_C (R_R + R_S) \tag{2}$$

By dividing both sides of Eq. (2) by R_S, the expression can be rewritten as follows:

$$\omega_S + \omega_R K = \omega_C (K + 1) \tag{3}$$

where K is the gear ratio of the ring gear to the sun gear, From Eqs. (1) $\sim$ (3), it can be found that the model in Fig. 2 (a) can form the traditional lever model of SPGS as the kinematic relationship among the sun gear, the carrier, and the ring gear can be described completely by Eq. (3). But, the kinematic information of planet gear cannot be represented in the traditional lever model since the terms related to the kinematic information of planet gear are eliminated during the process of merging similar items.

In Fig. 2 (b), the sun gear and carrier are rotating in different directions. Planet gear #1 is rotating in the opposite direction from the sun gear, and planet gear #2 is rotating in the same direction as the sun gear and ring gear. Therefore, the kinematic equations of the model in Fig. 2 (b) can be described as follows:

$$\begin{cases} V_{PA'} = \omega_C R_R - \omega_{P2} R_{P2} \\ V_{RA'} = \omega_R R_R \\ V_{PB'} = \omega_C R_S - \omega_{P1} R_{P1} \\ V_{SB'} = \omega_S R_S \\ V_{PC'} = \omega_{P1} R_{P1} = \omega_{P2} R_{P2} \end{cases} \tag{4}$$

where $V_{PA'}$ and $V_{RA'}$ represent the peripheral velocity at point A' of the planet gear and the ring gear of DPGS, respectively. $V_{PB'}$ and $V_{SB'}$ represent the peripheral velocity at point B' of the planet gear and the sun gear of DPGS, respectively. $V_{PC'}$ represents the peripheral velocity at point C' of planet gear #1 and planet gear #2. Similar expressions can be obtained as follows:

$$\omega_R R_R - \omega_S R_S = \omega_C (R_R - R_S) \tag{5}$$

$$\omega_R K - \omega_S = \omega_C (K - 1) \tag{6}$$

B. THE PROPOSED EXTENDED LEVER ANALOGY METHOD

The traditional LAM ignores the relationship between the planet gear and the lever model by eliminating the kinematic information of planet gear during the process of merging similar items. When the carrier is fixed and the sun gear is the driving component, the kinematic models are shown in Fig. 3 (a) and (b) for SPGS and DPGS respectively.

The kinematic relationship between planet gear, sun gear, and ring gear are established by eliminating the terms containing carrier speed, i.e. $\omega_C = 0$. In Fig. 3 (a), the planet gear and the ring gear are rotating in the same direction, and the sun gear is rotating in the opposite direction. The black arrows represent the translation of peripheral velocity at meshing points A and B. The deriving process of ALAM for SPGS can be written as follow:

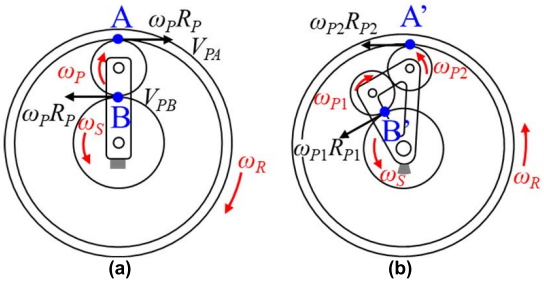

FIGURE 3. Kinematic model of the planetary gear set with the fixed carrier: (a) SPGS; (b) DPGS.

$$\begin{cases} \omega_S R_S = -\omega_P R_P \\ \omega_P R_P = \omega_R R_R \end{cases}, \quad \omega_C = 0 \tag{7}$$

where the expression containing the planet gear information is obtained:

$$\omega_R R_R - \omega_S R_S = 2\omega_P R_P \tag{8}$$

The assembly conditions of SPGS can be written as:

$$R_P = \frac{R_R - R_S}{2} \tag{9}$$

By substituting Eq. (9) into Eq. (8) and dividing both sides of Eq. (8) by R_S, the expression can be rewritten as follows:

$$\omega_R K/(K-1) - \omega_S/(K-1) = \omega_P \tag{10}$$

From Fig. 3 and Eq. (10), the kinematic relationship of the ALAM can be obtained.

In Fig. 3 (b), the sun gear, planet gear #2, and the ring gear are rotating in the same direction, but planet gear #1 is rotating in the opposite direction. The kinematic equations are different from that of the first method as follows:

$$\begin{cases} \omega_R R_R = \omega_{P2} R_{P2} \\ \omega_{P2} R_{P2} = -\omega_{P1} R_{P1} \\ \omega_S R_S = -\omega_{P1} R_{P1} \end{cases} \tag{11}$$

The above equations can be simplified as follows by applying the motion inversion to the carrier:

$$\begin{cases} \omega_R R_R = \omega_{P2} R_{P2} \\ \omega_S R_S = -\omega_{P1} R_{P1} \end{cases}, \quad \omega_C = 0 \tag{12}$$

The point location of planet gear in the ALAM can be determined by considering the relationship between rotating speeds and directions of SPGS components.

In Fig. 4, the white levers and nodes are the traditional LAM, and the black levers and orange nodes are the extended parts of the ALAM relative to the LAM (shown in Fig. 1).

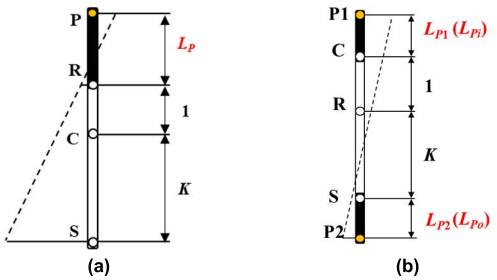

FIGURE 4. Initially extended lever model: (a) SPGS; (b) DPGS.

In terms of SPGS, the node of planet gear is located on the upper outside of the lever model of LAM, as shown in Fig. 4 (a). But, in terms of DPGS, the nodes of planet gears #1 and #2 are located on the upper and lower outsides of the lever model of LAM, respectively, as shown in Fig. 4 (b). It can be seen that the new nodes of planet gears exceed the research limitation of the traditional lever model of LAM and extend the LAM to the ALAM.

According to Eq. (10) and Fig. 4 (a), the lever model containing the information on the planet gear of SPGS can be written as follows:

$$\begin{cases} \dfrac{\omega_P}{\omega_R} = \dfrac{L_P + K + 1}{K + 1} = \dfrac{K}{K - 1} \\ \dfrac{\omega_P}{\omega_S} = \dfrac{L_P}{K + 1} = \dfrac{1}{K - 1} \end{cases} \tag{13}$$

Furthermore, the expression of the length for the new lever L_P of SPGS can be described as follows:

$$L_P = \frac{K + 1}{K - 1} \tag{14}$$

The new lever length of the planet gear in the ALAM is in good agreement with that of Reference [35].

Combining Eqs. (6), (11), and (12), the lever model containing the information of planet gears of DPGS can be written as follows:

$$\begin{cases} \dfrac{\omega_R}{\omega_{P2}} = \dfrac{R_{P2}}{R_R} \\ \dfrac{\omega_S}{\omega_{P1}} = -\dfrac{R_{P1}}{R_S} \\ \dfrac{\omega_{P1}}{\omega_{P2}} = -\dfrac{R_{P2}}{R_{P1}} \end{cases}, \quad \omega_C = 0 \tag{15}$$

Similarly, the expression of the length for the new lever L_{Pi} of DPGS can be described as follows:

$$\begin{cases} L_{P1} = (K + 1)\left(\dfrac{R_S}{R_{P1}}\right) \\ L_{P2} = \left(\dfrac{R_R}{R_{P2}}\right) - (K + 1) \end{cases} \tag{16}$$

The extended lever model can be obtained by substituting equations (14) and (16) into Fig. 4 (a) and (b), respectively, and describing the corresponding unknown lever length.

TABLE 1. Comparisons among the LAM and ALAM.

Information \ Method	LAM	ALAM
S (Sun gear)	△	△
R (Ring gear)	△	△
C (Carrier)	△	△
P (Planet gear)	X	△
Operability	△	△
Visualization	△	△
Speed sequence of PGSs/EGSs	X	△
All types of PGSs/EGSs	X	△

*△: covered, X: uncovered.

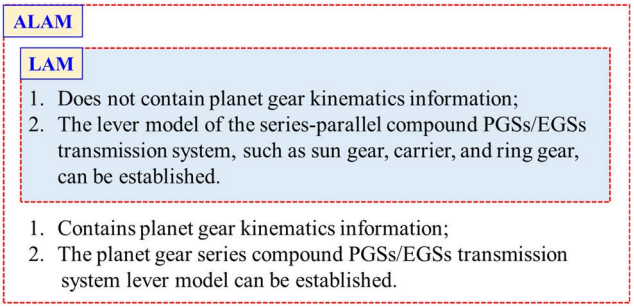

FIGURE 5. Significant difference between LAM and ALAM.

C. THE SUPERIORITY OF THE EXTENDED LEVER ANALOGY METHOD

It is well known that the traditional method (analysis method) is inefficient and cumbersome for analyzing the PGSs/EGSs by analyzing the kinematic of PGSs/EGSs in terms of torque and speed calculations. In addition, the abstraction of the equations and the complexity involved make many engineers unfamiliar with the specific functions and kinematic characteristics of complex PGSs/EGSs [36]. The LAM substitutes the torque and rotational speed relationship of the PGSs/EGSs components with the horizontal force and speed relationship of the lever node analogy. The kinematic functions of PGSs/EGSs are clearly visualized without entirely having a good command of the intricacies of PGSs/EGSs [5], [37].

Since the proposed ALAM is derived based on the LAM, the merits of LAM are also reflected in ALAM. The planet gear kinematic information needs to be considered for analyzing the planet gear life and the transmission efficiency of dual-input PGSs/EGSs. However, the traditional LAM cannot involves the kinematic information of planet gear. So the ALAM, in which the kinematic information of planet gear is included, becomes more significant. In addition, the unified equations and corresponding intuitively lever models are obtained readily by the proposed ALAM. Comparisons among the LAM and the ALAM for kinematic analysis of PGSs/EGSs in terms of containing components, operability, and visualization are shown in TABLE 1 and Fig. 5.

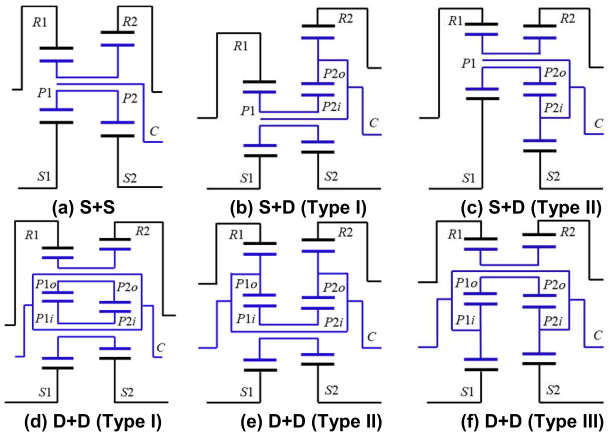

FIGURE 6. Schematic diagrams of the configurations which are beyond the analysis scope of LAM. Note: S+S, S+D, D+S, and D+D represent a transmission device that includes two PGSs/EGSs (SPGS and DPGS) and their distributions.

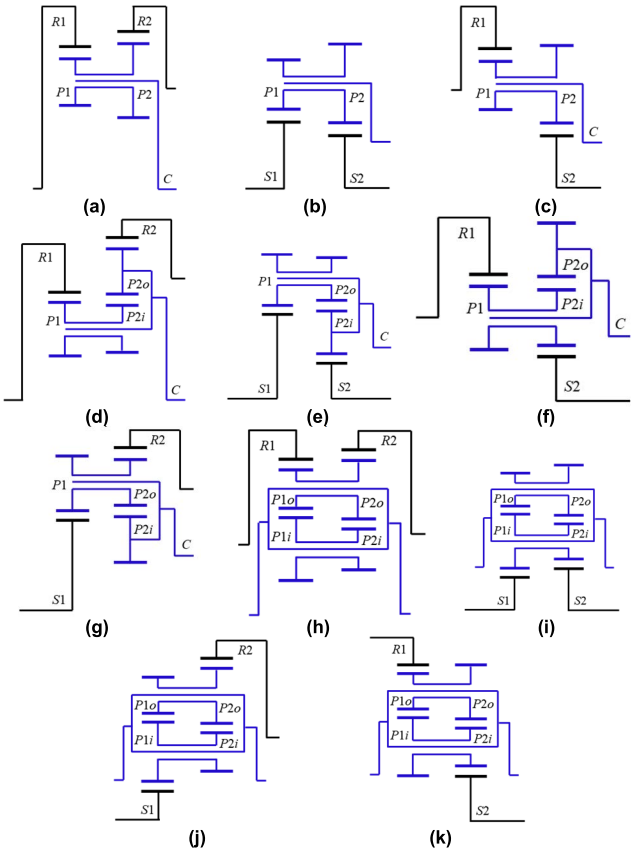

FIGURE 7. Derived 2K-H configurations of Fig 5: (a), (b), (c): S+S; (d), (e), (f), (g): S+D/D+S; (h), (i), (j), (k): D+D.

The compound PGSs/EGSs with planet gears in series are shown in Fig. 6, which are beyond the analysis scope of traditional LAM. Lots of the derived 2K-H configurations of Fig. 6 are obtained, which are shown in Fig. 7.

However, to establish the corresponding lever model, and analyze the speed ratio relationships and transmission efficiency under different schemes, it is necessary to solve and analyze the speed relationship between the planet gear and other components of PGSs/EGSs [2], [27], [38], [39], [40].

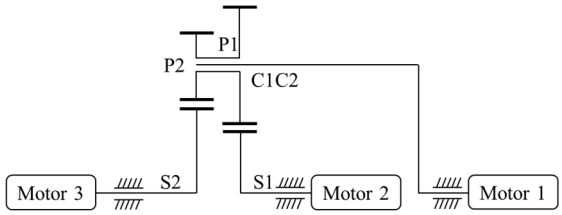

FIGURE 8. Schematic of epicyclic gear set proposed by NASA [41].

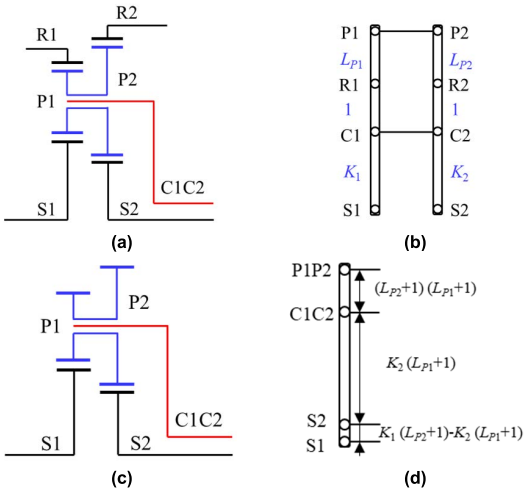

FIGURE 9. Mechanism and lever model for Fig. 8.

III. VALIDATION OF THE PROPOSED AUGMENTED LEVER ANALOGY METHOD

Figure 8 shows NASA's EGS mechanism [38], [41], [42], [43], namely the configuration of Fig. 7 (b), in which there are three links where the motor can be the input or the output. During the integration, the lever length between the planet gear and the ring gear is essential due to the specific structure of this mechanism. To analyze the kinematics of this mechanism conveniently based on the ALAM, the virtual PGSs/EGSs, and the corresponding extended lever models are established, as shown in Fig. 9 (a) and (b). According to Figs. 4 and 6, the mechanism diagram and virtual extended lever model can be integrated into a compound lever model, as shown in Fig. 9 (c) and (d) respectively, by using the improved lever analogy method proposed in Reference [33]. The teeth of the gears are as follows: $Z_{S1} = 28$, $Z_{P1} = 36$, $Z_{S2} = 36$, and $Z_{P2} = 28$. The speed ratio ω_{Ratio} between the components can be calculated by assuming that the virtual teeth of ring gear [44] are $Z_{R1} = Z_{S1} + 2Z_{P1}$, $Z_{R2} = Z_{S2} + 2Z_{P2}$.

$$R_{S1,S2}^{C1C2} = \frac{\omega_{S1}}{\omega_{S2}} = \frac{K_2 - 1}{K_1 - 1} = \frac{\frac{92}{36} - 1}{\frac{100}{28} - 1} = \frac{49}{81} \tag{17}$$

$$R_{S2,C1C2}^{S1} = \frac{\omega_{S2}}{\omega_{C1C2}} = \frac{K_1 - K_2}{K_1 - 1} = \frac{\frac{100}{28} - \frac{92}{36}}{\frac{100}{28} - 1} = \frac{32}{81} \tag{18}$$

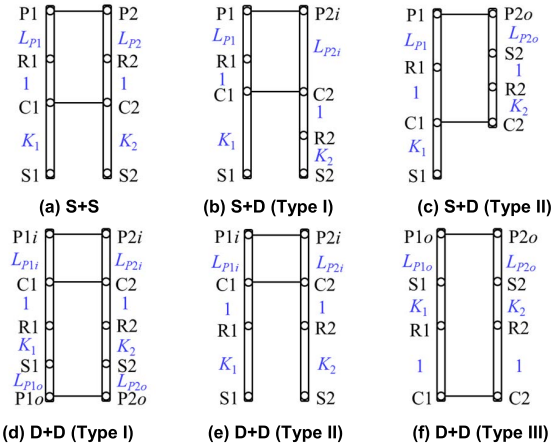

FIGURE 10. Schematic diagrams of the configurations beyond the analysis scope of LAM. Note: S+S, S+D, D+S, and D+D represent a transmission device that includes two PGSs/EGSs (SPGS and DPGS) and their distributions.

$$\omega_{S2} = \frac{49\omega_{S1}}{81} + \frac{32\omega_{C1C2}}{81} \tag{19}$$

$$R^{f}_{S1,S2} = \frac{\omega_{S1}}{\omega_{S2}} = \frac{49}{81} + \frac{32\omega_C}{81\omega_{S1}} \tag{20}$$

The results of the speed ratios of the mechanism in Fig. 8, i.e. Eqs. (17) and (20), are in good agreement with those of Reference [45], which verifies the accuracy of the ALAM. Compared to the traditional analysis method in References [41], [42], [43], [45], the kinematic equations of ALAM are easily visualized and understood without entirely having a good command of the intricacies of PGSs/EGSs. In addition, the example verifies the feasibility of the ALAM for the kinematic analysis of differential gear trains. The corresponding lever models of the configurations in Fig. 6 are shown in Fig. 10. The lever models of the configurations in Fig. 7 can be obtained by deleting the corresponding nodes of the lever models in Fig. 10.

IV. DUAL-INPUT ROTATING SPEED RELATION MODELING

A. SPGS MODELING EXAMPLE

Since all components in the dual-input working modes are rotating, the rotating speed relationship of the three components will affect the determination of the driving/driven part, and the direction of power flow in the system. Therefore, further discussion is required on a case-by-case basis. In the paper, the dual-input PGSs/EGSs are taken as a reduction device, and the working conditions are determined. In Fig. 11 (a), the red dotted arrows indicate the absolute rotating speed and direction of corresponding components. The blue dotted arrows indicate the output rotating speed and direction, which is relative to the carrier. During an upshift, ω_C rises and approaches ω_R. Here, ω_S-ω_C is a negative value, and ω_R-ω_C is a positive value. At this time, $\min(K/(1+K)) < \omega_C/\omega_R < 1$ and the transmission ratio $K \in [1.2, 4]$ [16] of the planetary gear mechanism should be considered as variables to solve the speed relationship of each component under this

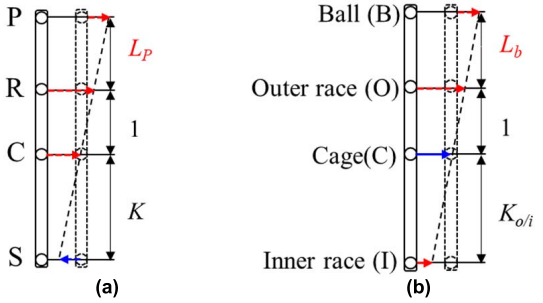

FIGURE 11. Extended lever model: (a) R-C dual-input of SPGS; (b) I-O dual-input of rolling bearing.

condition. The proposed method can also be applied to mechanisms with similar structures and kinematic characteristics, such as rolling bearings, etc, as shown in Fig. 11 (b). B, O, C, and I represent the balls, the outer race, the cage, and the inner race of the rolling bearing, respectively. L_b and $K_{o/i}$ respectively represent the lever length corresponding to the balls and the radii ratio of the outer race and inner race in rolling bearing. It is worth noting that there is only one dual-input working mode for rolling bearings (intermediate bearing), that is, the inner and outer races are the input parts, and the cage is the output part. Due to the limitation of space, this paper will not analyze the dual-input case of rolling bearings.

In Fig. 11 (a), the rotating speed of planet gear was calculated according to the two input rotating speeds, i.e. rotating speed of the ring gear and the carrier. Based on the ALAM, the speed ratios of the planet gear to the other three components can be written as Eq. (21) ∼ Eq. (24).

$$\omega_P = (\omega_S - \omega_C)(1 + L_P)\frac{1}{K} \tag{21}$$

$$\frac{\omega_P}{\omega_C} = \left(\frac{\omega_R}{\omega_C} - 1\right)(1 + L_P) \tag{22}$$

$$\frac{\omega_P}{\omega_R} = \left(1 - \frac{\omega_C}{\omega_R}\right)(1 + L_P) \tag{23}$$

$$\frac{\omega_P}{\omega_S} = \frac{1}{\frac{1}{\left(\frac{\omega_R}{\omega_C} - 1\right)(1+L_P)} - \frac{1}{1+L_P}} \tag{24}$$

B. DPGS MODELING EXAMPLE WITH PLANET GEAR #1 AND #2 HAVING THE SAME TOOTH NUMBER

1) R-C DUAL-INPUT DPGS MODELING

Figure 12 shows the extended lever model of DPGS, and the input components are the same as that in Fig. 12. Based on the ALAM, the speed ratios model of planet gears to the other three components can be expressed as Eq. (25) ∼ Eq. (29) while $Z_{P1} = Z_{P2}$.

$$\omega_{P1} = -(\omega_C - \omega_S)\frac{L_{P1}}{K+1} \tag{25}$$

$$\frac{\omega_{P1}}{\omega_C} = \left(1 - \frac{\omega_R}{\omega_C}\right)\frac{KL_{P1}}{K+1} \tag{26}$$

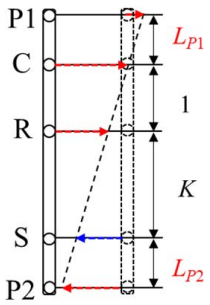

FIGURE 12. R-C dual-input extended lever model of the DPGS.

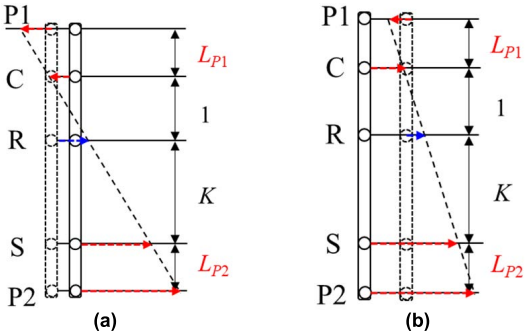

FIGURE 13. S-C dual-input extended lever model of the DPGS: (a) $\omega_C < 0$; $\omega_{P1} < 0$; (b) $\omega_C > 0$; $\omega_{P1} < 0$.

$$\frac{\omega_{P1}}{\omega_R} = \left(\frac{\omega_C}{\omega_R} - 1\right)\frac{KL_{P1}}{K+1} \tag{27}$$

$$\frac{\omega_{P1}}{\omega_S} = \frac{1}{\frac{1}{\left(1-\frac{\omega_R}{\omega_C}\right)\frac{KL_{P1}}{K+1}} + \frac{K+1}{KL_{P1}}} \tag{28}$$

$$\frac{\omega_{P1}}{\omega_{P2}} = -\frac{Z_{P2}}{Z_{P1}} \tag{29}$$

2) S-C DUAL-INPUT DPGS MODELING

Another extended lever model of DPGS with the input components being the carrier and the sun gear is shown in Fig. 13. Similarly, the speed ratios models of planet gears to the other three components can be expressed as Eq. (30) ∼ Eq. (33) based on the Eq. (6) and Eq. (16) while $Z_{P1} = Z_{P2}$. In this case, the rotating directions of the two inputs are in opposite directions, i.e. ω_C is negative and ω_S is positive, as shown in Fig. 13 (a). In the reverse operation of motors, ω_C is positive and increases from 0 to ω_S during upshift, as shown in Fig. 13 (b).

$$\omega_{P1} = (\omega_C - \omega_R)\, L_{P1} \tag{30}$$

$$\frac{\omega_{P1}}{\omega_C} = -\left(1 - \frac{\omega_S}{\omega_C}\right)\frac{L_{P1}}{K} \tag{31}$$

$$\frac{\omega_{P1}}{\omega_S} = \left(\frac{\omega_C}{\omega_S} - 1\right)\frac{L_{P1}}{K} \tag{32}$$

$$\frac{\omega_{P1}}{\omega_R} = \frac{1}{\frac{1}{-\left(1-\frac{\omega_S}{\omega_C}\right)\frac{L_{P1}}{K}} - \frac{1}{L_{P1}}} \tag{33}$$

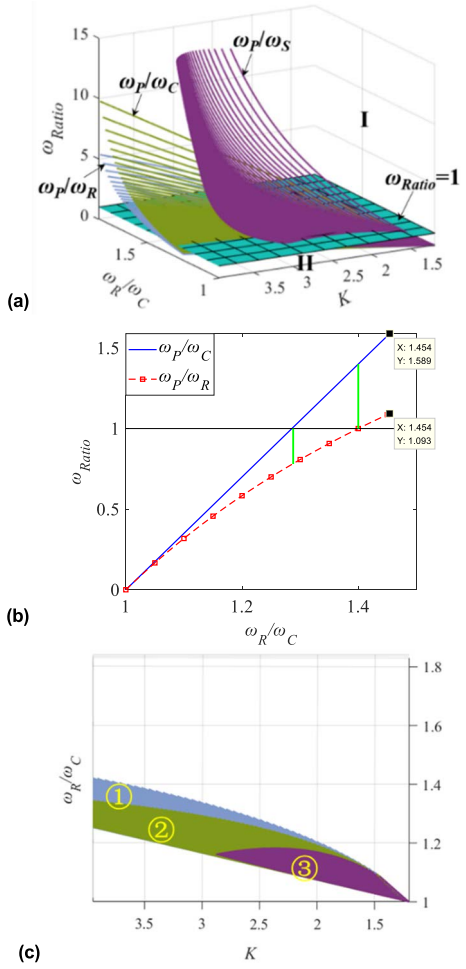

FIGURE 14. Speed ratios ω_P/ω_S, ω_P/ω_C and ω_P/ω_R: (a) The 3 dimension (D) view; (b) The 2D view of speed ratios ω_P/ω_C and ω_P/ω_R with changing ω_R/ω_C; (c) The top view while $\omega_{Ratio} \in [0, 1]$.

V. RESULTS AND DISCUSSION

In this section, the speed sequences between the components of the system with the different structures and input conditions are discussed.

A. SPGS R-C DUAL-INPUT

The relative rotating speed relationships between the planet gear and other components for SPGS are obtained by replacing Eq. (14) with Eqs. (21) ∼ (24), as illustrated in Fig. 14. Given parameters K and ω_R/ω_C, the speed ratios ω_P/ω_S, ω_P/ω_C, and ω_P/ω_R can be calculated readily, as shown in Fig. 14 (a). It can be found that the three speed ratios are increasing with K, but decreasing with ω_R/ω_C. To further describe the speed ratio relationship between ω_P and ω_S, ω_C and ω_R in Fig. 14 (a), the difference between two ratios ω_P/ω_C and ω_P/ω_R with $K = 2.2$, are demonstrated in Fig. 14 (b).

Since the values of ω_P/ω_C and the ω_P/ω_R are distributed on the upper and lower sides of $\omega_{Ratio} = 1$ respectively, like the region between two vertical lines shown in Fig. 14 (b) in which the values of ω_P/ω_C are larger than $\omega_{Ratio} = 1$, and

TABLE 2. Rotating speed relationships and speed sequence of R-C dual-input SPGS.

Region	Speed ratio relation				Speed sequence
	ω_P/ω_C	ω_P/ω_R	ω_R/ω_C	ω_P/ω_S	
I	>1	>1	>1	>1	$0<\omega_S<\omega_C<\omega_R<\omega_P$
II①	>1	<1	>1	>1	$0<\omega_S<\omega_C<\omega_P<\omega_R$
II②	<1	<1	>1	>1	$0<\omega_S<\omega_P<\omega_C<\omega_R$
II③	<1	<1	>1	<1	$0<\omega_P<\omega_S<\omega_C<\omega_R$

TABLE 3. Rotating speed relationships and speed sequence of R-C dual-input DPGS.

Region	Speed ratio relation				Speed sequence
	ω_{P1}/ω_C	ω_{P1}/ω_R	ω_{P1}/ω_S	ω_R/ω_C	
I	>1	>1	>1	<1	$\omega_{P2}<0<\omega_S<\omega_R<\omega_C<\omega_{P1}$
II①	<1	>1	>1	<1	$\omega_{P2}<0<\omega_S<\omega_R<\omega_{P1}<\omega_C$
II②	<1	<1	>1	<1	$\omega_{P2}<0<\omega_S<\omega_{P1}<\omega_R<\omega_C$
II③	<1	<1	<1	<1	$\omega_{P2}<0<\omega_{P1}<\omega_S<\omega_R<\omega_C$

the values of ω_P/ω_R are less than $\omega_{Ratio} = 1$. Therefore, Fig. 14 (a) is divided into two parts, i.e. part I and part II. To analyze the relationship between ω_P and ω_S, ω_C and ω_R, the sectional top view of Fig. 14 (a) with $\omega_{Ratio} = [0, 1]$, i.e. part II, is shown in Fig. 14 (c) in which ①: $0 < \omega_P/\omega_R < 1$, $\omega_P/\omega_C > 1, \omega_P/\omega_S > 1$; ②: $0 < \omega_P/\omega_R < 1, 0 < \omega_P/\omega_C < 1$, $\omega_P/\omega_S > 1$; ③: $0 < \omega_P/\omega_R < 1, 0 < \omega_P/\omega_C < 1$, $0 < \omega_P/\omega_S < 1$.

In Fig. 14 (c), part II is divided into three subparts and the speed sequences of the dual-input with the ring gear and carrier of SPGS are listed in TABLE 2.

B. DPGS R-C DUAL-INPUT

Based on the Eq. (16) and Eqs. (25) ∼ (29), the relative rotating speed relationship between the planet gear and other components for DPGS is illustrated in Fig. 15. The relationship between speed ratios ω_{P1}/ω_R, ω_{P1}/ω_C, and ω_{P1}/ω_S, which take ω_C/ω_R and Z_S/Z_{P1} as the variables, are shown in Fig. 15 (a). It can be found that the three speed ratios are increasing with both ω_C/ω_R and Z_S/Z_{P1}. The speed ratios ω_{P1}/ω_R, ω_{P1}/ω_C, and ω_{P1}/ω_S are illustrated in Fig. 15 (b) to (d), respectively. The different values of K affect the range and changing trend of the speed ratio. The maximum and minimum values occur at $K = 4$ and $K = 1.2$, respectively.

Similar to Fig. 14, Fig. 15 (a) is divided into four subparts. Part I and II are shown in 15 (a). The other parts, the sectional top view of Fig. 15 (a) with $\omega_{Ratio} = [0, 1]$, namely part II, are demonstrated in Fig. 15 (e) and (f) in which ①: $0 < \omega_{P1}/\omega_C < 1, \omega_{P1}/\omega_R > 1, \omega_{P1}/\omega_S > 1$; ②: $0 < \omega_{P1}/\omega_C < 1, 0 < \omega_{P1}/\omega_R < 1, \omega_{P1}/\omega_S > 1$; ③: $0 < \omega_{P1}/\omega_C < 1, 0 < \omega_{P1}/\omega_R < 1, 0 < \omega_{P1}/\omega_S < 1$. Three regions are changing between the limits with $K \in [1.2, 4]$.

Based on Fig. 15, the speed sequences of dual-input with the ring gear and the carrier of DPGS are listed in Table 3.

C. DPGS S-C DUAL-INPUT

Similarly, the relative rotating speed relationships for DPGS with the sun gear and the carrier as the input components can be obtained by substituting Eq. (16) into Eqs. (30) ∼ (33), as illustrated in Fig. 16. The relationship between speed ratios ω_{P1}/ω_R, ω_{P1}/ω_C, and ω_{P1}/ω_S, which take ω_C/ω_S and Z_S/Z_{P1} as the variables with K from 1.2 to 4., are shown in Fig. 16 (a) that is a general view. There are different changing trends of speed ratios with ω_C/ω_S and Z_S/Z_{P1}. The speed ratios

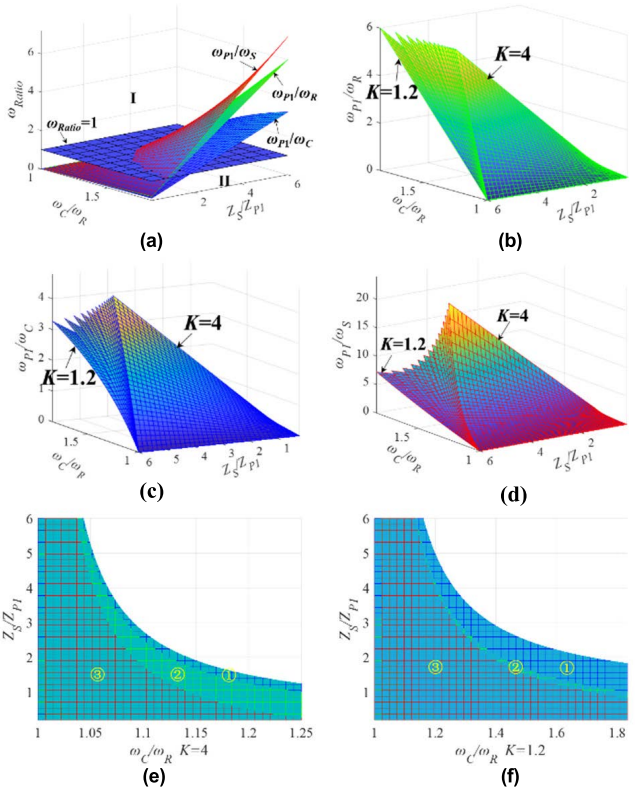

FIGURE 15. 3D view of speed ratios: (a) ω_{P1}/ω_S, ω_{P1}/ω_C and ω_{P1}/ω_R while $K = 1.2$; (b) ω_{P1}/ω_R; (c) ω_{P1}/ω_C; (d) ω_{P1}/ω_S. The top view of speed ratios ω_{P1}/ω_S, ω_{P1}/ω_C and ω_{P1}/ω_R while $\omega_{Ratio} \in [0,1]$: (e) $K = 4$; (f) $K = 1.2$.

TABLE 4. Rotating speed relationships and speed sequence of S-C dual-input DPGS.

Region		Speed ratio relation				Speed sequence
		ω_{P1}/ω_C	ω_{P1}/ω_R	ω_{P1}/ω_S	ω_{P2}/ω_S	
I		>1	<-1	>-1	<1	$\omega_{P1}<\omega_C<0<\omega_R<\omega_{P2}<\omega_S$
II①		>1	<-1	<-1	>1	$\omega_{P1}<\omega_C<0<\omega_R<\omega_S<\omega_{P2}$
II②	i	>-1	<-1	<-1	>1	$\omega_{P1}<0<\omega_C<\omega_R<\omega_S<\omega_{P2}$
	ii	>-1	>-1	<-1	>1	
	iii	>-1	>-1	>-1	<1	$\omega_{P1}<0<\omega_C<\omega_R<\omega_{P2}<\omega_S$
II③	i	<1	>1	<-1	>1	$\omega_{P1}<\omega_C<\omega_R<0<\omega_S<\omega_{P2}$
	ii	<1	>1	>-1	<1	$\omega_{P1}<\omega_C<\omega_R<0<\omega_{P2}<\omega_S$
	iii	<1	<1	>-1	<1	

ω_{P1}/ω_R, ω_{P1}/ω_C, and ω_{P1}/ω_S with $K = 4$ and $K = 1.2$ are illustrated in Fig. 16 (b). Fig. 16 (a) and (b) are divided

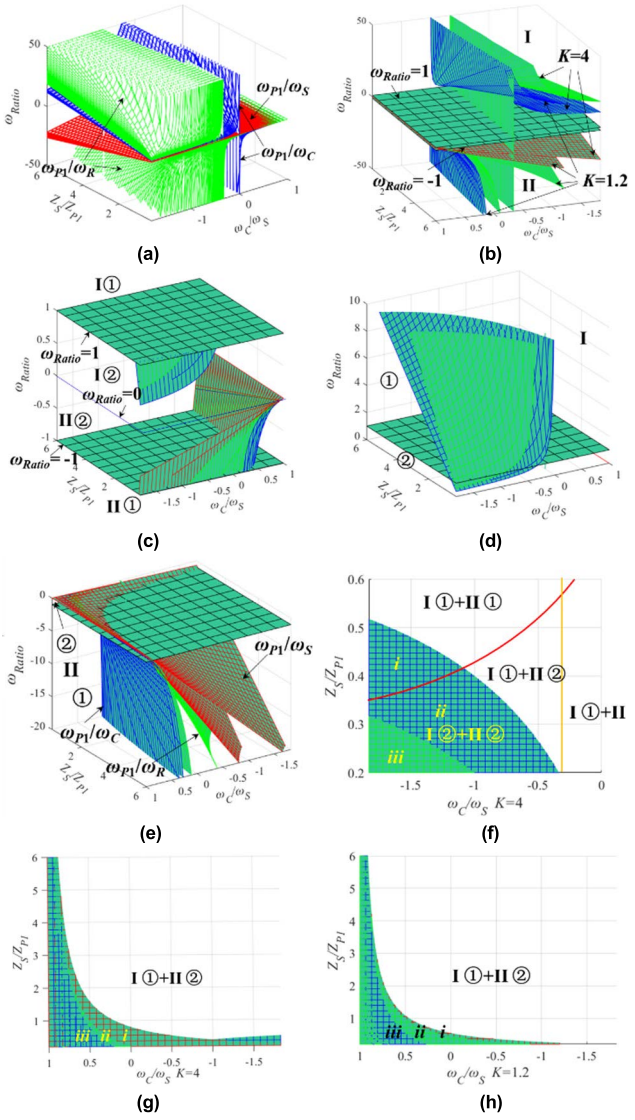

FIGURE 16. 3D view of speed ratios: (a) ω_{P1}/ω_S, ω_{P1}/ω_C, and ω_{P1}/ω_R; (b) rear view while $K = 1.2$ and $K = 4$; (c) $\omega_{Ratio} \in [-1, 0] \cap [0, 1]$; (d) $\omega_{Ratio} \geq 0$; (e) $\omega_{Ratio} \leq 0$. (f) The top view of speed ratios ω_{P1}/ω_S, ω_{P1}/ω_C and ω_{P1}/ω_R with $\omega_{Ratio} \in$ R while $K = 4$. The bottom view of speed ratios ω_{P1}/ω_S, ω_{P1}/ω_C and ω_{P1}/ω_R with $\omega_{Ratio} \in [-1, 0] \cap [0, 1]$: (g) $K = 4$; (h) $K = 1.2$.

into eight parts. Firstly, they are divided into two parts by the plane of $\omega_{Ratio} = 0$. Then, they are individually further divided into two subparts by planes of $\omega_{Ratio} = 1$ and $\omega_{Ratio} = -1$, respectively, as shown in Fig. 16 (c) to (e). Finally, the sectional top views of Fig. 16 (a) with $\omega_{Ratio} = [0, 1] \cap [-1, 0]$ are demonstrated in Fig.16 (f) to (h) in which *i*: $-1 < \omega_{P1}/\omega_C < 0$, $\omega_{P1}/\omega_R > 1$, $\omega_{P1}/\omega_S > 1$; *ii*: $0 < \omega_{P1}/\omega_C < 1$, $0 < \omega_{P1}/\omega_R < 1$, $\omega_{P1}/\omega_S > 1$; *iii*: $0 < \omega_{P1}/\omega_C < 1$, $0 < \omega_{P1}/\omega_R < 1$, $0 < \omega_{P1}/\omega_S < 1$. Since ω_{P1}/ω_R and ω_{P1}/ω_C are larger than 1 when $K = 1.2$, and the values of ω_{P1}/ω_R and ω_{P1}/ω_C follow hyperbolic function, so the other regions in Fig. 16 (f) are I①+II①, I①+II②, I①+II and I②+II② with $K = 4$.

The three regions in Fig.16 (g) and (h) are changing between the limits with $K \in [1.2, 4]$, respectively. Based on Fig. 16, the speed sequences of S-C dual-input DPGS are listed in TABLE 4.

VI. CONCLUSION

In this paper, an augmented lever analogy method containing the kinematic information of the planet gear was proposed. The lever node and length models of planet gear in planetary gear sets (PGSs/EGSs) were established by using the three instantaneous centers theorem to analyze the peripheral velocity of meshing points and make up for the lack in analyzing kinematic of planet gear and the compound PGSs/EGSs with planet gears in series of the traditional LAM caused by eliminating the kinematic information of planet gear during the process of merging similar items. The different dual-input working modes for PGSs/EGSs were carried out, and the rotating speed relationships and speed sequence between all components of SPGS (Simple planetary gear set) and DPGS (Double-planet planetary gear set) including the planet gears were obtained and discussed by divided regions. The main conclusion points of this study are drawn as follows:

1) The augmented lever analogy method (ALAM) was proposed by adding the nodes on the LAM to represent the planet gears, which can establish the lever model for all kinds of the PGSs/EGSs, and create new lever relationships of the planet gear to other components.
2) The proposed ALAM method has more significantly comprehensive merits including the newly unified kinematic expressions and intuitive and efficient analysis of all the components including the planet gears when compared to the traditional lever analogy method (LAM) while analyzing the kinematic information for the dual-input PGSs/EGSs.
3) The rotating speed relationships between components of PGSs/EGSs were divided into several regions within the variables range by taking the planes of ω_{Ratio} equal to 1 or -1. The corresponding regions and speed sequence can be found rapidly for PGSs/EGSs working at different modes.
4) It is worth noting that the mechanisms with similar structures and kinematic characteristics (e.g. compound PGSs/EGSs with planet gears in series, etc.) and planet-like mechanisms, (e.g. the rolling bearing), can also be analyzed by the proposed ALAM. Therefore, the proposed method is more general.

REFERENCES

[1] Y. G. Liao and M.-Y. Chen, "Analysis of multi-speed transmission and electrically continuous variable transmission using lever analogy method for speed ratio determination," *Adv. Mech. Eng.*, vol. 9, no. 8, Aug. 2017, Art. no. 168781401771294.
[2] R. G. Parker and J. Lin, "Mesh phasing relationships in planetary and epicyclic gears," *J. Mech. Design*, vol. 126, no. 2, pp. 365–370, Mar. 2004.
[3] L.-M. Wang and Y.-M. Shao, "Crack fault classification for planetary gearbox based on feature selection technique and *K*-means clustering method," *Chin. J. Mech. Eng.*, vol. 31, no. 1, pp. 242–252, Feb. 2018.

[4] Q. Xing, H. Yin, X. Zhao, and H. Zhang, "Research on schemes of multi-DOF planetary gearbox by combinatorial lever method," *Veh. Power Technol.*, vol. 129, no. 1, pp. 29–34, Jan. 2013.
[5] H. L. Benford and M. B. Leising, "The lever analogy: A new tool in transmission analysis," in *Proc. SAE Int. Cong. Expo.*, Detroit, MI, USA, Feb. 1981, pp. 429–437.
[6] H.-L. Xue, G. Liu, and X.-H. Yang, "A review of graph theory application research in gears," *Proc. Inst. Mech. Eng., C, J. Mech. Eng. Sci.*, vol. 230, no. 10, pp. 1697–1714, Jun. 2016.
[7] K. Ahn, S. Cho, W. Lim, Y.-I. Park, and J. M. Lee, "Performance analysis and parametric design of the dual-mode planetary gear hybrid power-train," *Proc. Inst. Mech. Eng., D, J. Automobile Eng.*, vol. 220, no. 11, pp. 1601–1614, Nov. 2006.
[8] W. Wang, R. Song, M. Guo, and S. Liu, "Analysis on compound-split configuration of power-split hybrid electric vehicle," *Mechanism Mach. Theory*, vol. 78, pp. 272–288, Aug. 2014.
[9] J. Kim, J. Kang, Y. Kim, T. Kim, B. Min, and H. Kim, "Design of power split transmission: Design of dual mode power split transmission," *Int. J. Automot. Technol.*, vol. 11, no. 4, pp. 565–571, Aug. 2010.
[10] T. Barhoumi, H. Kim, and D. Kum, "Compound lever based optimal configuration selection of compound-split hybrid vehicles," SAE Tech. Paper no. 2017-01-1148, Mar. 2017.
[11] T. Barhoumi, H. Kim, and D. Kum, "Automatic generation of design space conversion maps and its application for the design of compound split hybrid powertrains," *J. Mech. Des.*, vol. 140, no. 6, Mar. 2018, Art. no. 063401.
[12] H. Kim and D. Kum, "Comprehensive design methodology of input- and output-split hybrid electric vehicles: In search of optimal configuration," *IEEE/ASME Trans. Mechatronics*, vol. 21, no. 6, pp. 2912–2923, Dec. 2016.
[13] J. Kang, H. Kim, and D. Kum, "Systematic design of input- and output-split hybrid electric vehicles with a speed Reduction/Multiplication gear using simplified-lever model," *IEEE Trans. Intell. Transp. Syst.*, vol. 21, no. 9, pp. 3799–3810, Sep. 2020.
[14] X. Yang, N. Yue, Q. Yang, L. Wang, and H. Xiong, "Dynamic simulation for double input compound power-split mechanism of in-wheel motor driven EVs," *VDI Ber.*, vol. 2355, pp. 481–492, Sep. 2019.
[15] J. Liu, L. Yu, Q. Zeng, and Q. Li, "Synthesis of multi-row and multi-speed planetary gear mechanism for automatic transmission," *Mechanism Mach. Theory*, vol. 128, pp. 616–627, Oct. 2018.
[16] T. Xie, J. Hu, Z. Peng, and C. Liu, "Synthesis of seven-speed planetary gear trains for heavy-duty commercial vehicle," *Mechanism Mach. Theory*, vol. 90, pp. 230–239, Aug. 2015.
[17] G. Zhang, Z. Liu, J. Liu, and R. Song, "Design of two-row parallel planetary gear mechanism based on lever method," *J. Mech. Transmiss.*, vol. 42, no. 7, pp. 71–76, Jul. 2018.
[18] C. Ma, J. Ji, S. Ko, M. Song, J. Park, and H. Kim, "Comparative study on power characteristics and control strategies for plug-in HEV," in *Proc. IEEE Vehicle Power Propuls. Conf.*, Chicago, IL, USA, Sep. 2011, pp. 1–6.
[19] S. Hong, W. Choi, S. Ahn, Y. Kim, and H. Kim, "Mode shift control for a dual-mode power-split-type hybrid electric vehicle," *Proc. Inst. Mech. Eng. D, J. Automobile Eng.*, vol. 228, no. 10, pp. 1217–1231, Feb. 2014.
[20] F. Zhu, L. Chen, and C. Yin, "Design and analysis of a novel multimode transmission for a HEV using a single electric machine," *IEEE Trans. Veh. Technol.*, vol. 62, no. 3, pp. 1097–1110, Mar. 2013.
[21] T.-T. Ho and S.-J. Hwang, "Configuration synthesis of novel hybrid transmission systems using a combination of a Ravigneaux gear train and a simple planetary gear train," *Energies*, vol. 13, no. 9, p. 2333, May 2020.
[22] C. S. Ross and W. D. Route, "A method for selecting parallel-connected, planetary gear train arrangements for automotive automatic transmissions," in *Proc. SAE Passen. Conf. Expo.*, Nashville, TN, USA, Sep. 1991, pp. 1765–1774.
[23] C. Liu, J. Hu, Z. Peng, and S. Yang, "Analysis on three-mode configurations of power-split hybrid electric vehicle," in *Proc. 17th Int. Conf. Adv. Vehicle Technol., 12th Int. Conf. Design Educ., 8th Frontiers Biomed. Devices*, Boston, MA, USA, Aug. 2015, Paper DETC2015-46754, V003T01A042.
[24] Z.-X. Peng, J.-B. Hu, T.-L. Xie, and C.-W. Liu, "Design of multiple operating degrees-of-freedom planetary gear trains with variable structure," *J. Mech. Design*, vol. 137, no. 9, Sep. 2015, Art. no. 093301.
[25] E. L. Esmail, E. Pennestrì, and A. H. Juber, "Power losses in two-degrees-of-freedom planetary gear trains: A critical analysis of Radzimovsky's formulas," *Mechanism Mach. Theory*, vol. 128, pp. 191–204, Oct. 2018.
[26] D. Rabindran and D. Tesar, "Parametric design and power-flow analysis of parallel force/velocity actuators," *J. Mech. Robot.*, vol. 1, no. 1, Feb. 2009, Art. no. 011007.
[27] C. Wang, B. Dong, and R. G. Parker, "Impact of planet mesh phasing on the vibration of three-dimensional planetary/epicyclic gears," *Mechanism Mach. Theory*, vol. 164, Oct. 2021, Art. no. 104422.
[28] L. Niu, H. Cao, Z. He, and Y. Li, "An investigation on the occurrence of stable cage whirl motions in ball bearings based on dynamic simulations," *Tribol. Int.*, vol. 103, pp. 12–24, Nov. 2016.
[29] H. Liu, H. Liu, C. Zhu, and R. G. Parker, "Effects of lubrication on gear performance: A review," *Mechanism Mach. Theory*, vol. 145, Mar. 2020, Art. no. 103701.
[30] F. Meng, H. Han, Z. Ma, and B. Tang, "Effects of aviation lubrication on tribological performances of graphene/MoS_2 composite coating," *J. Tribol.*, vol. 143, no. 3, Aug. 2020, Art. no. 031401.
[31] Y. Luo, W. Tu, C. Fan, L. Zhang, Y. Zhang, and W. Yu, "A study on the modeling method of cage slip and its effects on the vibration response of rolling-element bearing," *Energies*, vol. 15, no. 7, p. 2396, Mar. 2022.
[32] Y. Li, S. Li, J. Zhang, and Q. Dang, "Discussion on the design of bearing of planetary gear for dual-mode cutting reducer," *J. Mech. Transmiss.*, vol. 42, no. 7, pp. 77–80, Jul. 2018.
[33] X. Yang, Y. Shao, L. Wang, W. Yu, N. Yue, and W. Du, "Configuration design of dual-input compound power-split mechanism for in-wheel motor-driven electrical vehicles based on an improved lever analogy method," *J. Mech. Design*, vol. 143, no. 10, Apr. 2021, Art. no. 104501.
[34] O. Munteanu, "Dynamic modelling and simulation of a planetary speed increaser," *Bull. Transilvania Univ. Brasov. Eng. Sci.*, vol. 9, no. 58, pp. 27–34, 2016.
[35] P. Attibele, "A new approach to understanding planetary gear train efficiency and powerflow," *SAE Int. J. Adv. Current Pract. Mobility*, vol. 2, no. 6, pp. 3180–3188, 2020.
[36] R. Reddy and I. Rajasri, "Velocity analysis of EGTs: Lever analogy method," *Int. J. Sci. Res. Develop.*, vol. 3, no. 12, pp. 797–799, 2016.
[37] G. Liao, "Using lever analogy diagrams in teaching compound planetary gear trains," in *Proc. Annu. Conf. Expo.*, Chicago, IL, USA, Jun. 2006, pp. 11.1393.1–11.1393.11.
[38] E. L. Esmail, "Meshing efficiency analysis of two degree-of-freedom epicyclic gear trains," *J. Mech. Des.*, vol. 138, no. 8, Jun. 2016, Art. no. 083301.
[39] E. Pennestrì, L. Mariti, P. P. Valentini, and V. H. Mucino, "Efficiency evaluation of gearboxes for parallel hybrid vehicles: Theory and applications," *Mechanism Mach. Theory*, vol. 49, pp. 157–176, Mar. 2012.
[40] E. L. Esmail, "Influence of the operating conditions of two-degree-of-freedom planetary gear trains on tooth friction losses," *J. Mech. Des.*, vol. 140, no. 5, May 2018, Art. no. 054501.
[41] L. D. Webster, "Rotary drive mechanism accepts two inputs," *NASA Tech. Briefs*, vol. 11, no. 5, p. 11325, May 1987.
[42] C. Chen and J. Chen, "Efficiency analysis of two degrees of freedom epicyclic gear transmission and experimental validation," *Mechanism Mach. Theory*, vol. 87, pp. 115–130, May 2015.
[43] E. Pennestrı and P. P. Valentini, "A review of formulas for the mechanical efficiency analysis of two degrees-of-freedom epicyclic gear trains," *J. Mech. Des.*, vol. 125, no. 3, pp. 602–608, Sep. 2003.
[44] R. Mathis and Y. Remond, "Kinematic and dynamic simulation of epicyclic gear trains," *Mechanism Mach. Theory*, vol. 44, no. 2, pp. 412–424, Feb. 2009.
[45] H. A. Hussen, E. L. Esmail, and R. A. Hussen, "Power flow simulation for two-degree-of-freedom planetary gear transmissions with experimental validation," *Model. Simul. Eng.*, vol. 2020, no. 6, Nov. 2020, Art. no. 8837605.

XIAODONG YANG received the M.D. degree in mechanical engineering from Henan Polytechnic University, Jiaozuo, China, in 2015. He is currently pursuing the Ph.D. degree in mechanical engineering with Chongqing University, Chongqing, China. His current research interests include mechanical design, mechanical systems, dynamic modeling, data analysis, and electric vehicles powertrain design and control.

WENNIAN YU received the M.Sc. degree in mechatronic engineering from Chongqing University, Chongqing, China, and the Ph.D. degree in mechanical engineering from Queen's University, Kingston, Canada. He is currently a Research Fellow at Chongqing University. His research interests include dynamic modeling of gear transmission systems, condition monitoring of gear system for diagnostics, prognostics and health management, and remaining useful life estimation of mechanical systems using machine learning and deep learning algorithms.

YIMIN SHAO received the B.S. degree in metallurgical machinery from the University of Science and Technology, Beijing, China, in 1992, and the Ph.D. degree in production engineering from Gunma University, Japan, in 1997. From 1997 to 2004, he was a Research Associate with the Gunma University, and a Visiting Scholar with the EU FP7 Marie Curie International Incoming Fellow, U.K., in 2012. He is currently a Professor and the Vice Director with the State Key Laboratory of Mechanical Transmissions, Chongqing University, Chongqing, China. His research interests include signal processing, noise analysis, pattern recognition, equipment fault diagnosis, intelligent monitoring, and residual life prediction.

ZHILIANG XU received the B.S. degree in mechanical engineering from the Anhui University of Science and Technology, China, in 2014. He is currently pursuing the Ph.D. degree in mechanical engineering with Chongqing University, China. His research interests include mechanical systems, dynamic modeling, equipment fault diagnosis, data analysis, and pattern recognition.

QIANG ZENG received the B.S. and Ph.D. degrees in mechanical engineering from Chongqing University, Chongqing, China. He was sponsored by the China Scholarship Council's joint Ph.D. Program as a joint Ph.D. at the University of Huddersfield. He is currently a Research Associate in mechanical engineering at the State Key Laboratory of Mechanical Transmissions, Chongqing University. His research interests include signal processing, equipment fault diagnosis, data analysis, and pattern recognition.

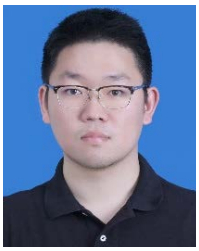

CHUNHUI NIE received the B.S. degree in mechanical engineering from Chongqing Jiaotong University, China, in 2014. He is currently pursuing the Ph.D. degree in mechanical engineering with Chongqing University, China. His research interests include hybrid energy storage unit, hydraulic hybrid energy recovery systems, equipment fault diagnosis, data analysis, and pattern recognition.

DINGQIANG PENG received the B.S. degree in mechanical engineering from the University of Science and Technology, Beijing, China, in 2009. He is currently pursuing the Ph.D. degree in mechanical engineering with Chongqing University, China. His research interests include manufacturing automation, precision engineering, and signal processing.